AN INTEGRATED MICROFLUIDIC PLATFORM FOR IN-SITU CELLULAR CYTOKINE SECRETION IMMUNOPHENOTYPING

Nien-Tsu Huang[1], Weiqiang Chen[1], Bo-Ram Oh[1], Jianping Fu[1,2] and Katsuo Kurabayashi[1,3]

[1]Mechanical, [2]Biomedical, and [3]Electrical Engineering, University of Michigan, Ann Arbor, Michigan, USA

ABSTRACT

Rapid, quantitative detection of cell-secreted biomarker proteins with a low sample volume holds great promise to advance cellular immunophenotyping techniques for diagnosis and treatment of infectious diseases. Here we successfully developed an immunophenotyping assay with THP-1 human moncytic leukemia cells using a highly integrated microfluidic platform incorporating a no-wash bead-based chemiluminescence immunodetection scheme. Our study achieved ultra-sensitive cellular immunophenotyping with 20-fold fewer cells and 7 times faster than the conventional enzyme-linked immunosorbent assay (ELISA). Our strategy of monitoring immune cell functions could impact medical treatments of infectious diseases by enabling a sample-efficient cellular immunophenotyping analysis.

KEYWORDS

Cellular immunophenotyping, Microfluidics, Optics, Chemiluminescence.

INTRODUCTION

Cell-stimulation assay is a well-accepted technique for functional immunophenotyping analysis in immune disease diagnosis.[1, 2] It involves triggering immune response of white blood cells by introducing a stimulant followed by quantitatively measurements of cell-secreted cytokines (*e.g.*, TNF-α). Conventional methods to quantify cellular cytokine production by enzyme-linked immunosorbent assay (ELISA) [3] usually require a large reagent volume and numerous manual manipulation and laborious and time-consuming processes, preventing using ELISA for clinical decision-making under time pressure. To overcome the limitations of conventional functional immunophenotyping methods using ELISA, we developed a polydimethylsiloxane (PDMS)-based microfluidic immunophenotyping assay (MIPA) device (Fig. 1a) capable of integrating all the assay operations on a single chip, including cell seeding, cell stimulation, and cell-secreted cytokine detection. The MIPA device incorporated a surface-micromachined PDMS microfiltration membrane (PMM). The MIPA device with the PMM provided a well-confined and miniaturized microenvironment for cell seeding and stimulation and permitted rapid diffusion of cell-secreted cytokine molecules from the cell culture chamber to the immunoassay chamber as illustrated in Fig. 1b. The miniaturized size of the MIPA device required less sample volume and shortened cytokine diffusion time. Our biomarker detection scheme further employed a bead-based chemiluminescence assay requiring no washing and lysing step while conjugating cell-secreted cytokines with assay beads, which enabled in-situ cell-secreted cytokine detections with the MIPA device. We used a canonical stimulant, lipopolysaccharide (LPS), to trigger functional responses of immune cells such as cytokine production.[4] The cytokine of interest to this work is tumor necrosis factor-α (TNF-α), a pro-inflammatory cytokine and a key biomarker associated with host defense and immunosurveillance.[5] TNF-α secretion from LPS-stimulated immune cells has been shown to reflect a functioning innate immune response. The MIPA device demonstrated here eliminated a need for complex instrumental operations, prolonged sample pretreatments, and protein surface immobilizations. Using the MIPA device, we demonstrated a rapid, convenient, and reagent-saving functional immunophenotyping assay with only 1,000 cells required, which is 20-fold less than required by current cell-stimulation assays. Owing to the miniaturized microenvironment coupled with no-wash bead-based homogenous immunoassay, the total assay time required for all the cell loading, cell stimulation, reagent incubation, and detection processes in the MIPA device was only about 3.5 hr, 7 times faster than needed for conventional ELISA assay.

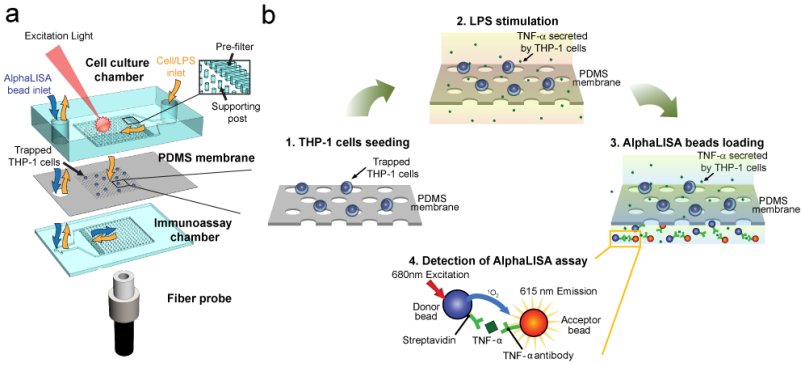

Figure 1 Design and operation of the MIPA device. (a) Schematic of the multi-layered MIPA device. (b) SEM image of the PMM (c) Schematic of the functional immunophenotyping assay protocol.

EXPERIMENT

The structure of the MIPA device consisted of three different PDMS layers. The top and bottom PDMS layers were the cell culture and immunoassay chambers, respectively, and the middle layer was a PMM. The top cell culture chamber

of the MIPA device was designed for seeding and stimulation of THP-1 cells using LPS. The bottom immunoassay chamber of the MIPA device was designed for loading immunoassay beads and optical detection of AlphaLISA signals. The PMM was embedded between the top and bottom microfluidic layers for (1) isolation and enrichment of THP-1 cells and (2) allowing cytokines secreted from LPS-stimulated cells to diffuse rapidly into the bottom immunoassay chamber for quantitative immunosensing. The PMM contained an array of closely packed through holes of 4 μm in diameter and with a center-to-center distance of 10 μm. The PMM had an effective filtration area of 7 mm^2 and a thickness of 10 μm. The cell isolation and cytokine diffusion efficiency is critically dependent on the membrane porosity, which is defined as the ratio between the total pore area to the total membrane area. In this work, we successfully fabricated the PMM with 25% porosity. Even with the high porosity of the PMM, we did not observe any deformation of the PMM during all cell loading experiments, suggesting the PMM structure has superior mechanical robustness owing to the PMM supporting structures integrated in both the cell culture and immunoassay chambers. We characterized the cell seeding performance of the MIPA device for on-chip isolation and enrichment of THP-1 cells. THP-1 cells of 10-30 μm in diameter were loaded into the MIPA device in the complete cell medium at three different concentrations of 1×10^5, 5×10^5, 1×10^6 cells/mL under a flow rate of 5 μL/min. Fig. 2a&b show a photograph of the MIPA device and a SEM image of the PMM. Fig. 2c represents a temporal sequence of false-colored brightfield images showing isolation and enrichment of THP-1 cells on the PMM. Using these brightfield images, we quantified the cell seeding density on the PMM as a function of the sample loading volume (Fig. 2d). Our results in Fig. 2 demonstrate that we could conveniently control the total number of THP-1 cells trapped on the PMM by modulating the sample injection time, necessary for normalizing the amount of TNF-α secreted by single THP-1 cells.

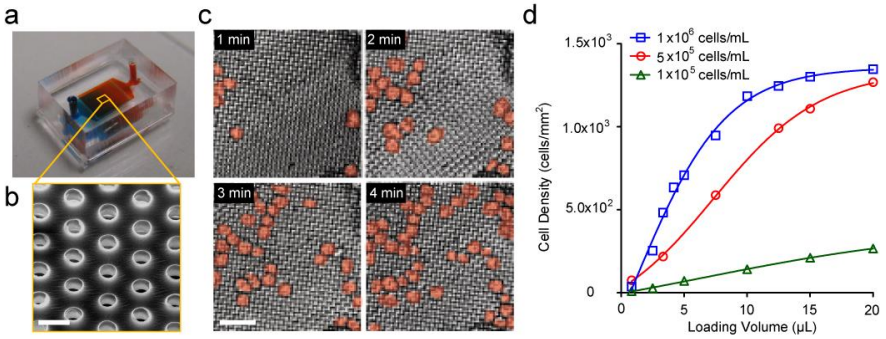

Figure 2 Isolation and enrichment of THP-1 cells using the MIPA device. (a) Sequence of false-colored brightfield cell seeding images at different time points. (b) Plot of trapped cells density on the PMM as a function of loading volume.

We systematically quantified the levels of TNF-α secreted by THP-1 cells as a function of the total cell population trapped on the PMM (n = 1,000, 5,000, and 20,000 cells) and the LPS concentration (10, 50, 100 ng/mL). The AlphaLISA signal detected using the optical system was converted to the TNF-α concentration using a TNF-α standard curve (Fig. 3a) generated using AlphaLISA with samples spiked with known concentrations of TNF-α. This TNF-α standard curve provided a correlation between the TNF-α concentration in the MIPA device and the corresponding AlphaLISA signal intensity. Fig. 3b plotted the TNF-α concentration secreted by THP-1 cells as a function of the total cell population and the LPS concentration. Our result demonstrated that as expected, the concentration of TNF-α secreted by THP-1 cells increased according to both the cell number and the LPS concentration. When the LPS concentration increased from 10 to 100 ng/mL, the TNF-α concentration secreted by 1,000, 5,000 and 20,000 THP-1 cells increased from 53 to 80 pg/mL, 67 to 123 pg/mL and 150 to 528 pg/mL, respectively. Fig. 3c&d plotted the average amount of TNF-α secreted by single THP-1 cells as a function of LPS concentrations (Fig. 3c) or the amount of LPS molecules available to single THP-1 cells (Fig. 3d). As shown in Fig. 3c, the amount of TNF-α secreted by single THP-1 cells appeared to increase as the cell number decreased. More interestingly, as shown in Fig. 3d, the amount of TNF-α secreted by single THP-1 cells for different cell densities (n = 1,000, 5,000, and 20,000) collapsed and followed a single linear positive trend with the amount of LPS molecules available to single THP-1 cells, suggesting that TNF-α secretion process by single THP-1 cells might be dictated by the available LPS molecules independent of the cell population size. Finally, we compared the levels of TNF-α secretion between normal and deactivated THP-1 cells that were both stimulated with LPS. Identifying deactivation of monoctyes (also termed as immunoparalysis) can provide an effective means to predict health risks such as development of infectious complications.[6] It is believed that real-time phenotypic identification of patients with immunoparalysis could be used to guide alternative care strategies, such as immune stimulation.[7] To examine whether the MIPA device could distinguish normal THP-1 cells vs. immunoparalyzed immune cells, THP-1 cells were first treated with the complete cell growth medium supplemented with 10 ng/mL LPS for 24 hr to attenuate their secretion of cytokines, including TNF-α, in response to a second LPS stimulation. Deactivated THP-1 cells were then loaded into the MIPA device for TNF-α secretion measurements. Fig. 3e compared TNF-α concentrations secreted by normal and deactivated THP-1 cells trapped on the PMM for n = 20,000 cells. Consistent with prior in vitro models, TNF-α secretion by deactivated THP-1 cells was 2-4 times less than those of normal THP-1 cells, especially when LPS concentration was greater than 50 ng/mL. More interestingly, deactivated THP-1 cells appeared to be not sensitive to changes of LPS concentration as compared to normal THP-1 cells, as concentrations of the TNF-α secreted by deactivated THP-1 cells remained roughly constant (105 ± 12 pg/mL) as LPS concentration increased from

10 to 100 ng/mL. In distinct contrast, concentrations of TNF-α secreted by normal THP-1 cells increased from 150 to 528 pg/mL with LPS concentration increasing from 10 to 100 ng/mL.

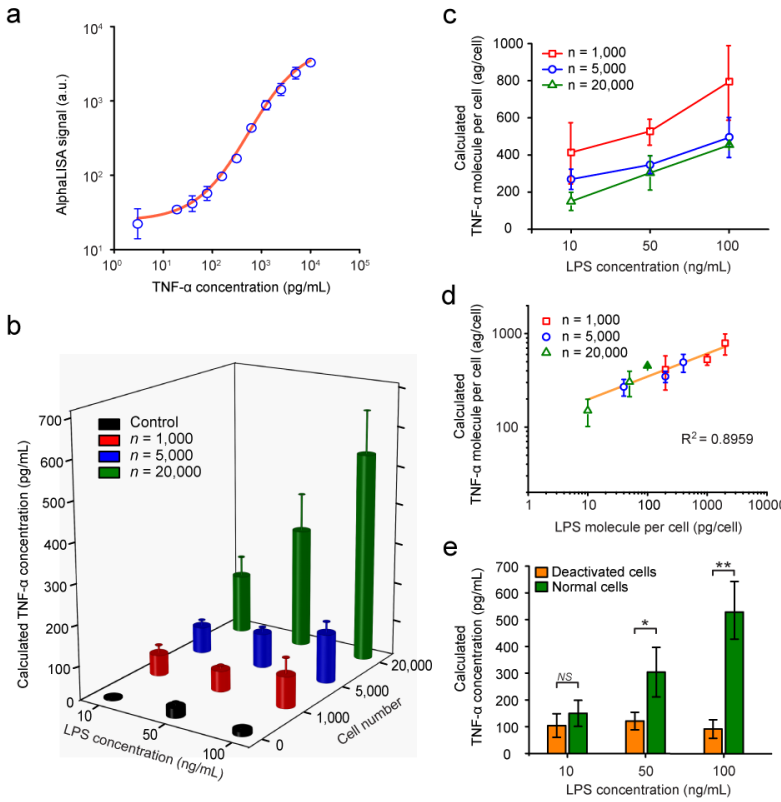

Figure 3 Detection of TNF-α secreted from LPS-stimulated THP-1 cells using the MIPA device. (a) Standard curve for TNF-α detection. (b) Plot of TNF-α concentration secreted by LPS-stimulated THP-1 cells as a function of total cell number and LPS concentration. (c) Plot of TNF-α concentration secreted by normal and LPS-deactivated THP-1 cells. (d&e) Plots of TNF-α concentration secreted by individual cells as a function of LPS concentration (d) or LPS concentration per cell (e).

CONCLUSION

In summary, we demonstrated a rapid, convenient, and reagent-saving functional immunophenotyping assay using the MIPA device with only 1,000 cells required. Owing to the miniaturized microenvironment coupled with no-wash bead based homogenous immunoassay, the total assay time including LPS stimulation and AlphaLISA detection was only about 3.5 hr, 7 times faster than the conventional ELISA-based assay. Our MIPA device might find great applications in infectious and inflammatory disease diagnosis with only small sample volumes required and rapid assay time for clinical decision-making under time pressure.

REFERENCES

[1] J. S. Boomer, *et al.*, "Immunosuppression in patients who die of sepsis and multiple organ failure," *JAMA*, vol. 306, pp. 2594-605, (2011).

[2] T. T. Cornell, *et al.*, "Clinical implications and molecular mechanisms of immunoparalysis after cardiopulmonary bypass," *J Thorac Cardiovasc Surg*, vol.143, pp.1160-1161, (2011).

[3] J. H. Cox, *et al.*, "Measurement of cytokine release at the single cell level using the ELISPOT assay," *Methods*, vol. 38, pp. 274-82, (2006).

[4] E. Louis, *et al.*, "Tumour necrosis factor (TNF) gene polymorphism influences TNF-alpha production in lipopolysaccharide (LPS)-stimulated whole blood cell culture in healthy humans," *Clin Exp Immunol*, vol. 113, pp. 401-6, (1998).

[5] W. Shurety, *et al.*, "Localization and post-Golgi trafficking of tumor necrosis factor-alpha in macrophages," *J Interferon Cytokine Res*, vol. 20, pp. 427-38, (2000).

[6] M. Azizia, *et al.*, "Immune Status in Very Preterm Neonates," *Pediatrics*, vol. 129, pp. 967-974, (2012).

[7] M. W. Hall, *et al.*, "Immunoparalysis and nosocomial infection in children with multiple organ dysfunction syndrome," *Intensive Care Med*, vol. 37, pp. 525-32, (2011).

CONTACT

Katsuo Kurabayashi katsuo@umich.edu, Jianping Fu jpfu@umich.edu